

Electro-acoustic hysteresis behaviour of PZT thin film bulk acoustic resonators

M. Schreiter*, R. Gabl, D. Pitzer, R. Primig, W. Wersing

Siemens AG, Corporate Technology, CT MM 2, D-81730 Munich, Germany

Abstract

Thin film bulk acoustic resonators (FBARs) based on $\text{Pb}(\text{Zr}_x\text{Ti}_{1-x})\text{O}_3$ (PZT) with varying compositions, ranging from $x = 0.25$ to 0.6, were fabricated to investigate hysteresis-like dependencies of the resonance frequency and electro-mechanical coupling constant on bias voltage. The resonators, formed by a simple sandwich structure consisting of bottom electrode, PZT thin film and top electrode, arranged on a planar acoustic mirror, were designed to give a resonance frequency of about 2 GHz. PZT thin films were deposited in a planar multi target sputtering system using three metallic targets in a reactive Ar/O_2 mixture. For low Zr-content, where PZT is grown in the tetragonal phase, the parallel resonance frequencies are strongly dependent on the applied electric field, while the series resonance frequency is practically unaffected. This behaviour is completely different for rhombohedral PZT at higher Zr-content. Here the series resonance frequency becomes strongly field dependent, which can be attributed to $109^\circ/71^\circ$ domain switching. As a potential application based on the observed strong field dependence of the acoustic properties, a bandwidth-tuneable or programmable RF filter based on PZT FBARs is proposed.

© 2003 Elsevier Ltd. All rights reserved.

Keywords: FBAR; Ferroelectric properties; PZT

1. Introduction

Recently, thin film bulk acoustic resonators (FBARs) have seen a remarkable amount of interest for their use in narrow band RF filters. Their small size, low cost and high quality factors give them the potential to replace SAW filters currently used in mobile communication systems. The active component of an FBAR consists of a piezoelectric thin film, typically AlN or ZnO. However, ferroelectric materials, e.g. $\text{Pb}(\text{Zr}_x\text{Ti}_{1-x})\text{O}_3$ (PZT), are also, in general, suitable.

Piezoelectricity in ferroelectrics arises from a linearization of the electrostrictive effect due to spontaneous polarisation.¹ Regarding thickness mode excitation of a polycrystalline thin film, the effective piezoelectric stress coefficient e_{33}^* results from the superposition of the single domain contributions, i.e. e_{33}^* is determined by the net macroscopic polarisation which follows the ferroelectric hysteresis, $P(E)$. In addition, the effective electro-mechanical coupling coefficient k_t^{*2} , for thickness mode excitation, is related to e_{33}^{*2} as follows:

$$k_t^{*2} = \frac{e_{33}^{*2}}{c_{33}^{*D} \cdot \epsilon_{33}^{*S}} \quad (1)$$

where c_{33}^{*D} and ϵ_{33}^{*S} are the according effective stiffness coefficient and permittivity, respectively. Consequently, resonance characteristics, in particular electro-mechanical coupling and resonance frequency are expected to exhibit a hysteresis-like bias dependency.

Some papers have already considered the effect of poling on resonance characteristics.^{3,4} However, although the above described bias dependency of acoustic properties has been extensively studied for bulk material, these effects have hardly been addressed with regards to FBARs yet.

The purpose of this paper is to introduce and discuss the results of comprehensive investigations on the electro-acoustic behaviour of PZT thin film resonators with varying compositions and to introduce a possible new application arising from that.

2. Sample preparation and experimental

PZT thin films were reactively deposited in a multi-target sputtering system from 3 metallic targets (Pb, Zr

* Corresponding author.

E-mail address: matthias.schreiter@siemens.com (M. Schreiter).

and Ti) in a 50/50 Ar/O₂ mixture. The substrate temperature and sputtering pressure were fixed at 525 °C and 0.4 Pa, respectively. The film thickness ranged between 350 and 425 nm to produce a resonance frequency of about 2 GHz.

As substrates, 4 inch silicon wafers covered with an acoustic $\lambda/4$ -mirror to decouple resonators from the substrate and a Pt bottom electrode, were used. This mirror is realised by a 3-fold stack of alternating Pt and ZnO layers having a high and low acoustic impedance, respectively. During PZT deposition the substrates rotate permanently over the targets, thus the film grows sequentially layer by layer in the ferroelectric perovskite phase, i.e. no thermal treatment after deposition is needed.

The Zr content x of $\text{Pb}(\text{Zr}_x\text{Ti}_{1-x})\text{O}_3$ was varied between 0.25 (PZT25/75) and 0.6 (PZT60/40) simply by changing the power delivered to the individual targets. Thus both thin films of the tetragonal and rhombohedral phase were realised. As reported earlier,⁵ films of these compositions show significant differences concerning self polarisation, permittivity and hysteresis characteristics, making them interesting for electroacoustic hysteresis studies.

A top layer of Au with a thickness of 100 nm was deposited onto the PZT film and patterned to give test resonators with different sizes ($30 \times 30 \mu\text{m}^2$ up to $500 \times 500 \mu\text{m}^2$). For frequencies of 2 GHz the ground signal is capacitively coupled to the bottom electrode. Fig. 1 gives a ground plot of such a test structure. To enable a bias voltage to be supplied, the bottom electrode was uncovered at one spot on the wafer and connected to the ground by wire bonding.

Capacity, loss tangent and C(V)-behaviour at 10 kHz were measured using an LCR-meter. RF characterisations of resonators were performed using a network analyser. Standard RF on-wafer measurement techniques were employed. Both LCR-meter and network analyser were equipped with a voltage source used for biasing.

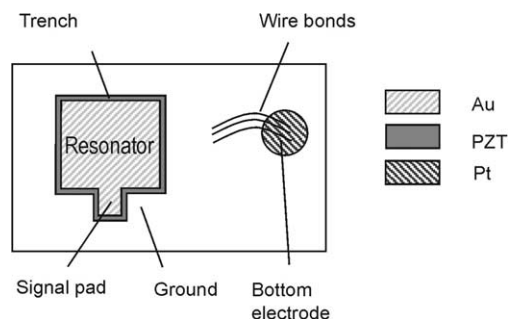


Fig. 1. Schematic plot of a resonator structure: The part of the top Au layer denoted as ground is connected to the bottom electrode by wire bonding.

3. Results

XRD analysis revealed a strong preferred (111)-orientation, independent of the film composition. Pyrochlore was not observed.

According to earlier investigations,⁶ C(V)-characteristics strongly depend on the film composition. Fig. 2 shows the derived $\epsilon_r(E)$ -plots for films with different Zr-contents. For PZT25/75 $\epsilon_r(E)$ is significantly asymmetric and strongly shifted by an internal bias voltage. An applied negative voltage will be in alignment with the direction of self polarisation, from bottom to top. The effect of the self polarisation is especially strong for Zr-contents < 30%.⁶ Thus for PZT25/75 the maximum of ϵ_r in the negative virgin curve is significantly degenerated, indicating that nearly no domain switching occurs due to self polarisation. The higher the Zr content, the weaker the described effects. For PZT58/42, $\epsilon_r(E)$ displays a rather more symmetric shape and the internal bias has almost disappeared. As in bulk material, the coercive field strength E_c becomes smaller with higher Zr contents. It should be noted that the virgin permittivity of 285 for PZT25/75 is significantly increased to 685 for PZT58/42. A summary of ϵ_r for different compositions is given in Table 1. In addition, the ratio between maximum and minimum permittivity considerably increases with higher Zr-content from about 1.5 (PZT25/75) to more than 4 (PZT58/42).

Typical impedance vs. bias characteristics of $70 \times 70 \mu\text{m}^2$ resonators based on PZT25/75 are presented in Fig. 3. Dependent on the bias, spurious responses

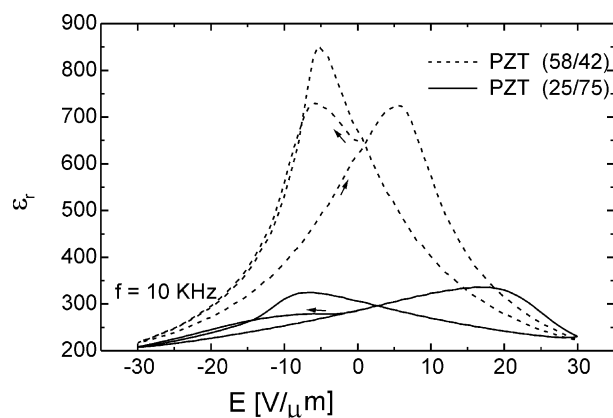


Fig. 2. Permittivity vs. electric field derived from C(V) behaviour measured on PZT thin films with varying compositions.

Table 1
Summary of ϵ_r and maximum k_t for different PZT compositions

	PZT (25/75)	PZT (34/66)	PZT (44/56)	PZT (52/48)	PZT (58/42)
ϵ_r	285	380	600	665	685
k_t	0.21	0.23	0.28	0.295	0.3

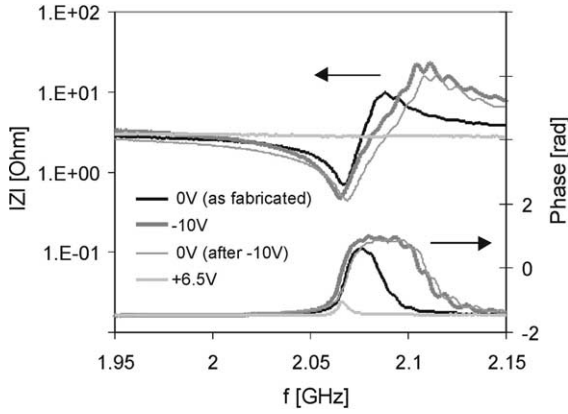


Fig. 3. Measured impedance of a $(70 \times 70) \mu\text{m}^2$, PZT25/75 based resonator for different bias voltages. Due to self polarisation the virgin curve shows typical resonance behaviour.

become more prominent for lower sizes. For larger resonators the series resonance starts to degenerate due to series resistances. As the sample is self polarised the virgin resonator shows a significant resonance behaviour. Typical values for Q-factors derived from the Butterworth-Van Dyke equivalent circuit² of a resonator amount to 220 for the series resonance of the virgin $70 \times 70 \mu\text{m}^2$ resonator. As expected, the electrical bias has an enormous impact on the resonance characteristics. The effective coupling constant can be varied between zero, i.e. there is no piezoelectric response due to a zero net polarisation, and a maximum value of about 0.21. For higher Zr-content this value increases and achieves its maximum for PZT58/42 at about 0.3. The results for maximum coupling coefficients achieved for different compositions are summarised in Table 1.

Fig. 4 shows the series and parallel resonance frequencies vs. bias voltage for tetragonal and rhombohedral PZT resonators. The weakening of self polarisation and decreasing of the coercive field strength with increasing Zr-content are consistent with the C(V)-behaviour. For tetragonal PZT25/75 the parallel resonance shows a strong bias dependence, whereas the series resonance is nearly unaffected. This behaviour is completely changed for rhombohedral PZT58/42, where the series resonance frequency is mainly controlled by the bias. However, the influence on the parallel resonance is rather weak.

Worth mentioning but not explicitly shown here, is that for compositions near the morphotropic phase boundary where the tetragonal and rhombohedral phase are co-existing, a hysteresis is observed for both series and parallel resonances.

Eqs. (2) and (3) give the relations for the parallel and series resonance of an FBAR in thickness mode excitation:²

$$f_p = \frac{1}{2t} \sqrt{\frac{c_{33}^{*D}}{\rho}} \approx \frac{1}{2t} \sqrt{\frac{c_{33}^{*E}}{\rho}} \cdot \frac{1}{1 - 0.5k_t^{*2}} \quad (2)$$

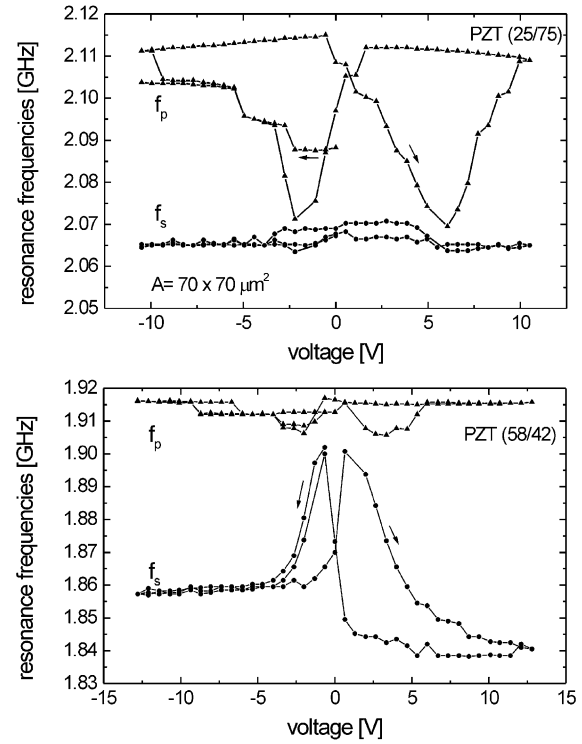


Fig. 4. Resonance frequency vs. bias voltage for PZT FBARs with varying compositions.

$$f_s = f_p \sqrt{1 - \frac{8}{\pi^2} k_t^{*2}} \approx \frac{1}{2t} \sqrt{\frac{c_{33}^{*E}}{\rho}} \cdot \frac{1 - 0.41k_t^{*2}}{1 - 0.5k_t^{*2}} \quad (3)$$

where ρ and t are density and thickness of the film. Considering (111)-oriented films, only the angle θ between the direction of polarisation and the normal to the surface is determined. In-plane the domains are randomly oriented. An estimation of c_{33}^{*E} can be achieved by averaging over the domain orientation in the film assuming $c_{33}^{*E} \approx \langle c_{33}^{*E} \rangle$ where $\langle c_{33}^{*E} \rangle$ represents the averaged stiffness coefficient. In particular, transforming the compliance matrix s , which can be evaluated using the Devonshire theory, with respect to θ supplies the averaged compliance coefficients $\langle s_{\alpha\beta}^E \rangle$ initially. In the following $\langle c_{33}^{*E} \rangle$ can be evaluated using the relationship: $c^E = (s^E)^{-1}$.

As illustrated in Fig. 5, for the tetragonal case, $|\theta|$ is either 54.74° or 125.26° . Since the transformation equations for the compliance, a forth rank tensor, contain $(\cos \theta)$ to even powers only, the elastic behaviour, specifically c_{33}^{*E} , is independent of the direction of the polarisation. Thus, according to Eq. (2), f_p reduces significantly around E_c when the polarisation is switched since the coupling constant approaches zero due to a vanishing of the net polarisation. In other words, f_p drops due to reduced piezoelectric stiffening if domains are switched. According to (3) f_s is almost independent of k_t^{*2} . These conclusions are in a good agreement with

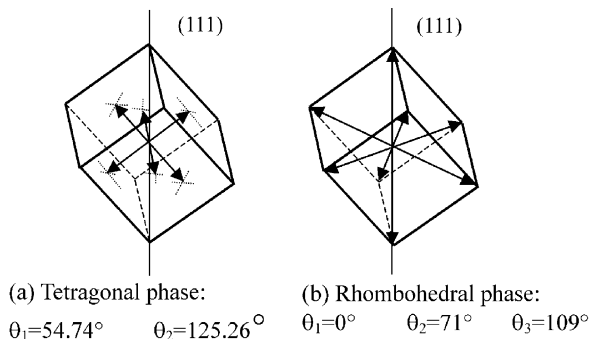


Fig. 5. Possible domain orientation in tetragonal (a) and rhombohedral (b) (111)-oriented films. θ Refers to the angle between polarisation vector and the normal to the surface given by the (111)-direction.

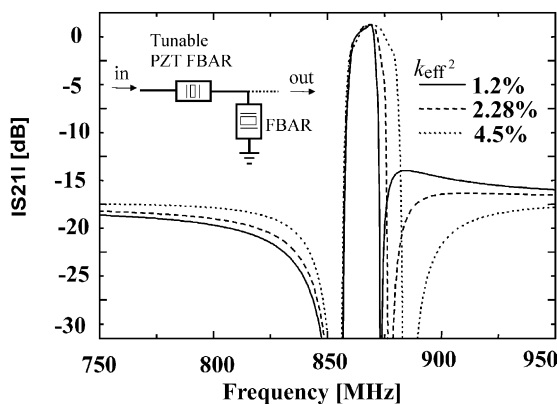


Fig. 6. Simulation results for $|S_{21}|$ of a three-fold ladder filter, where the series acoustic resonator is realised by a tuneable PZT FBAR with $Q = 500$ and low Zr content.

the measured results. For the rhombohedral phase the situation is different. As shown in Fig. 5, $|\theta|$ amounts to either 0° , 71° or 109° . Hence, the transformation of the compliance matrix generally delivers different results for $71^\circ/109^\circ$ domains or 0° domains. As seen in earlier investigations, due to tensile stress a certain number of the domains are $71^\circ/109^\circ$ domains.⁵ If this number increases during switching, c_{33}^*E will be expected to change around E_c . Considering measured results with respect to Eqs. (2) and (3), c_{33}^*E is supposed to increase. This compensates the effect of reduced piezoelectric coupling around E_c , leading to a significant bias dependency of f_s and weakening the bias dependency of f_p . Indeed, a qualitative estimation based on the above described domain averaging using compliance coefficients derived from Devonshire theory, confirms that c_{33}^*E can increase for $71^\circ/109^\circ$ domains compared to 0° domains confirming the altered relationship between the resonance frequencies and bias, in the rhombohedral case.

As a potential application, taking advantage of the described bias controlled resonance properties, a ladder filter based on FBARs is considered. If at least one

resonator is ferroelectric (Fig. 6), the bandwidth of the filter becomes tuneable according to the altered frequency separation between parallel and series resonance frequencies by controlling k_t^2 . Simulation results for $|S_{21}|$ of a three-fold ladder filter are given in Fig. 6.

These filters could be used for adaptive discrimination of channels and/or limiting noise bandwidth. Furthermore because of the polarisation present after poling, one can think about PZT FBAR programmable filters where once, by poling, filter parameters are adjusted, but during operation no bias is applied.

4. Summary and conclusions

Investigations of the bias dependency of the resonance behaviour of PZT FBARs with varying compositions revealed a significant hysteresis-like change in the coupling constant and resonance frequencies according to the ferroelectric hysteresis. This effect has to be carefully taken into account if ferroelectric thin films are to be considered for the application in FBARs. The coupling-coefficient was found to increase with the Zr-content. For tetragonal PZT, the parallel resonance drops significantly around E_c which is due to a decrease of piezoelectric stiffening. However, f_s is hardly affected by biasing. For rhombohedral compositions the series resonance becomes significantly bias dependent. It is suggested that this is due to an additional stiffening if a significant portion of the domains are of the $71^\circ/109^\circ$ type around E_c combining with the effect of reduced piezoelectric coupling.

As a potential application taking advantage of the investigated electro-acoustic effect, a ladder filter containing at least one ferroelectric FBAR is introduced enabling a bias controlled or even programmable filter bandwidth.

References

1. Sonin, A. S. and Strukow, B. A., *Einführung in die Ferroelektrizität*. Akademie Verlag, Berlin, 1974 (pp. 151).
2. Rosenbaum, J. F., *Bulk Acoustic Wave Theory and Devices*. Artech House Inc, Norwood, 1988.
3. Hanajima, N., Tsutsumi, S., Yonezawa, T., Hashimoto, K., Nanjo, R. and Yamaguchi, M., Ultrasonic properties of lead zirconate titanate thin films in UHF-SHF range. *Jpn. J. Appl. Phys.*, 1997, **36**, 6069–6072.
4. Kirby, P., Komuro, Eiju., Imura, M., Zhang, Q., Su, Q. and Whatmore, R., High frequency thin film ferroelectric acoustic resonators and filters. *Integrated Ferroelectrics*, 2001, **41**, 91–100.
5. Wersing, W. and Bruchhaus, R., *Pyroelectric Devices and Applications, Handbook of Thin Film Devices*. Academic Press, 2000 (pp. 143–201).
6. Schreiter, M., Bruchhaus, R., Pitzer, D. and Wersing, W., Sputtering of self-polarised PZT films for IR detector arrays. *Proceedings of ISAF XI*, 1998.